EBioMedicine 18 (2017) 146–156

Contents lists available at ScienceDirect

EBioMedicine

journal homepage: www.ebiomedicine.com

Research Paper

Clock Gene Dysregulation Induced by Chronic ER Stress Disrupts β-cell Function

Yasuharu Ohta [a,b,*,1], Akihiko Taguchi [a,1], Takuro Matsumura [a], Hiroko Nakabayashi [a], Masaru Akiyama [a], Kaoru Yamamoto [a], Ruriko Fujimoto [a], Risa Suetomi [a], Akie Yanai [c], Koh Shinoda [c], Yukio Tanizawa [a,*]

[a] Department of Endocrinology, Metabolism, Hematological Science and Therapeutics, Yamaguchi University, Graduate School of Medicine, 1-1-1, Minami Kogushi, Ube, Yamaguchi 755-8505, Japan
[b] Department of Diabetes Research, Yamaguchi University, School of Medicine, 1-1-1, Minami Kogushi, Ube, Yamaguchi 755-8505, Japan
[c] Department of Neuroanatomy, Yamaguchi University, Graduate School of Medicine, 1-1-1, Minami Kogushi, Ube, Yamaguchi 755-8505, Japan

ARTICLE INFO

Article history:
Received 16 January 2017
Received in revised form 9 March 2017
Accepted 27 March 2017
Available online 30 March 2017

Keywords:
Endoplasmic reticulum stress
Clock out-put gene
Diabetes mellitus
Pancreatic islet β-cell
Insulin secretion

ABSTRACT

In *Wfs1*$^{-/-}$ *A*^{y}*/a* islets, in association with endoplasmic reticulum (ER) stress, *D-site-binding protein* (*Dbp*) expression decreased and *Nuclear Factor IL-3* (*Nfil3*)/E4 *Promoter-binding protein 4* (*E4bp4*) expression increased, leading to reduced DBP transcriptional activity. Similar alterations were observed with chemically-induced ER stress. Transgenic mice expressing E4BP4 under the control of the mouse *insulin I* gene promoter (MIP), in which E4BP4 in β-cells is expected to compete with DBP for D-box, displayed remarkable glucose intolerance with severely impaired insulin secretion. Basal ATP/ADP ratios in MIP-E4BP4 islets were elevated without the circadian oscillations observed in wild-type islets. Neither elevation of the ATP/ADP ratio nor an intracellular Ca2+ response was observed after glucose stimulation. RNA expressions of genes involved in insulin secretion gradually increase in wild-type islets early in the feeding period. In MIP-E4BP4 islets, however, these increases were not observed. Thus, molecular clock output DBP transcriptional activity, susceptible to ER stress, plays pivotal roles in β-cell priming for insulin release by regulating β-cell metabolism and gene expressions. Because ER stress is also involved in the β-cell failure in more common Type-2 diabetes, understanding the currently identified ER stress-associated mechanisms warrants novel therapeutic and preventive strategies for both rare form and common diabetes.

1. Introduction

Wolfram syndrome, caused by the WFS1 mutation and characterized by insulin-dependent diabetes mellitus and optic atrophy, is a prototypical human endoplasmic reticulum (ER) disease (Akiyama et al., 2009; Fonseca et al., 2005; Inoue et al., 1998; Ueda et al., 2005; Yamada et al., 2006). Genetic mutations in pro-insulin genes or Unfolded Protein Response (UPR) component genes also cause inherited diabetes accompanied by islet β-cell ER stress in both rodents and humans (Delépine et al., 2000; Harding et al., 2000). In addition, recent studies have suggested that glucotoxicity and lipotoxicity induce ER stress responses resulting in β-cell failure (Pretty and Nolan, 2006; Bachar et al., 2009). While the mechanism underlying the loss of β-cell function is still a matter of debate, ER stress is believed to contribute to the onset and the progression of type-2 diabetes (T2DM).

T2DM is characterized by loss of β-cell function and mass, resulting from interactions between genetic predisposition and various environmental factors (Cornelis and Fu, 2012). One environmental condition that is increasingly being recognized as a risk factor for T2DM is circadian rhythm disruption (Nilsson et al., 2004; Pan et al., 2011), and various animal studies support the concept that clock genes have essential functions in the endocrine pancreas (Marcheva et al., 2010; Perelis et al., 2015). The correlation between circadian disruption and T2DM is partly attributable to β-cell failure, though the mechanisms remain largely unknown. *Clock* mutant mice exhibited altered expressions of genes known to regulate islet growth, survival, maturation, and proliferation (Marcheva et al., 2010), and a recent study provided evidence that stimulation of light-induced circadian misalignment recapitulates the metabolic and molecular defects observed in β-cell specific clock gene mutants (Qian et al., 2013). *Bmal1* deletion in β-cells also resulted in failed metabolic adaptation to a high fat-diet, which was characterized by hyperglycemia, glucose intolerance and loss of glucose-stimulated insulin secretion (Rakshit et al., 2016). Our previous results indicated that down-regulation of the *albumin D-site-binding protein* (*Dbp*) and

* Corresponding authors at: Department of Endocrinology, Metabolism, Hematological Science and Therapeutics, Yamaguchi University, Graduate School of Medicine, 1-1-1, Minami Kogushi, Ube, Yamaguchi 755-8505, Japan.
E-mail addresses: yohta@yamaguchi-u.ac.jp (Y. Ohta), tanizawa@yamaguchi-u.ac.jp (Y. Tanizawa).
[1] Equal contributors.

http://dx.doi.org/10.1016/j.ebiom.2017.03.040

up-regulation of the *Nfil3* (*Nuclear Factor IL-3*)/E4 *Promoter-binding protein 4* (*E4bp4*) contribute to direct suppression of Aryl hydrocarbon receptor nuclear translocator (ARNT) expression in the diabetic state (Nakabayashi et al., 2013). β-cell failure caused by β-cell clock disruption could, at least in part, be a consequence of decreased DBP transactivity followed by decreased expressions of genes involved in β-cell secretory function and mass.

Sleep disturbances contribute to the risks of developing several diseases including diabetes and obesity, and studies have demonstrated that *Bip*, the negative regulator of the ER stress response, is up-regulated in the cerebral cortex and hypothalamus following acute sleep loss/deprivation (Mackiewicz et al., 2007; Cirelli and Tononi, 2004). However, the molecular mechanisms linking circadian clock function with β-cell ER stress remain unknown.

Wfs1$^{-/-}$ *A*^{y}*/a* is an animal model of Wolfram syndrome with mild obesity. Herein, we demonstrated DBP transcriptional activity to be profoundly reduced in *Wfs1*$^{-/-}$ *A*^{y}*/a* islets and that similar alterations were observed in ER stress-induced MIN6 cells and islets. Transgenic mice, in which β-cells overexpressing E4BP4 would be expected to compete with DBP for D-box, displayed remarkable β-cell failure associated with sustained elevation of the basal ATP/ADP ratio and failure of this ratio to rise in response to glucose stimulation. In addition, the expressions of several genes linked to insulin secretion were suppressed. Our findings clearly demonstrate the importance of clock genes in insulin secretion, and ER stress may dysregulates these clock genes. ER stress is involved in many cellular processes including insulin secretion. Circadian clocks have also recently been identified as playing pivotal roles in pancreatic islet β-cell function. Herein, we set out to address the hypothesis that β-cell circadian clock dysregulation is a critical component of ER stress-induced β-cell failure. Elucidating the role of circadian clocks in ER stress-induced β-cell failure may lead to the development of novel tools for the prevention and treatment of diabetes.

2. Materials and Methods

2.1. Mouse Experiments

All experimental protocols were approved by the Ethics of Animal Experimentation Committee at Yamaguchi University School of Medicine. The animals were housed in a temperature-controlled (24 °C ± 1 °C) room under a 12-h light: 12-h dark cycle (LD12: 12). Zeitgeber time (ZT) 0 was designated as lights on and ZT 12 as lights off. The high-fat diet (rodent diet with 60% energy from fat; D12492) was purchased from Research Diet (New Brunswick, NJ).

2.2. Cell Culture and Islet Culture

MIN6 cells were maintained as a monolayer in 25 mM glucose Dulbecco's modified Eagle's medium complemented with 15% fetal calf serum and 71.5-μM β-mercaptoethanol. The MIN6 cells used were from 23 to 30 cell passages. MIN6 cells were equilibrated with 5% CO_2 at 37 °C and supplemented with 50 mg/l streptomycin and 75 mg/l penicillin sulfate. Islets of Langerhans were isolated from C57BL/6 mice by ductal perfusion with collagenase. The intact islets were handpicked and maintained in RPMI medium supplemented with 10% fetal calf serum for 24 h prior to the experiments.

2.3. Generation of Mouse Insulin I Gene Promoter – E4BP4 – Transgenic Mice

The mouse *insulin I* gene promoter (MIP)-GFP-transgenic construct was kindly provided by Dr. M. Hara, University of Chicago. The MIP-E4BP4-transgenic construct was created by replacing GFP-cDNA with mouse E4BP4 (mE4BP4)-cDNA (1744 bp; ATCC) at the *XhoI* site. The 12.2-kb MIP-mE4BP4-human growth hormone (hGH) fragment was isolated from the vector by digestion of the plasmid construct with *SfiI* and *HindIII*. The purified transgene DNA was microinjected into the pronuclei of C57BL/6 mice by UNITECH Company (Chiba, Japan). Genotyping was performed by PCR using DNA isolated from tail snips. The resulting offspring were screened for transgene transmission by PCR analysis and Southern hybridization. Two different mouse lines were maintained and littermates were used in the experiments.

2.4. Western Blot Analysis

The nuclear proteins from isolated islets were extracted using the NE-PER Nuclear and Cytoplasmic Extraction Reagent Kit (Pierce) according to the manufacturer's instructions. Protein concentrations were determined employing a BCA Kit (Pierce) according to the manufacturer's instructions. Two to four micrograms of nuclear protein samples were separated by SDS-PAGE and transferred to nitrocellulose membranes (GE Healthcare). The membranes were then incubated with antibodies. Antibodies against E4BP4 (sc-28,203) and LAMIN B (sc-6216) were purchased from Santa Cruz Biotechnology.

2.5. RNA Isolation and Real-time RT-PCR

Total RNA extraction from MIN6 cells was performed with the RNeasy Mini Kit (Qiagen). Total RNA extraction from mouse islets was performed with both Isogen (Nippon Gene) and the RNeasy Mini Kit. cDNA was synthesized with Superscript II Reverse Transcriptase (Life Technologies) and subjected to real-time PCR using Power SYBR Green PCR Master Mix (Life Technologies) on an ABI 7300 HT thermal cycler (Life Technologies). The value of each cDNA was calculated using the ΔCt method and normalized to the value of the housekeeping gene, *Gapdh*. The sequences of the primers were as follows:

m*Dbp* forward: 5′-CTTTTGACCCTCGGAGACAC-3′.
m*Dbp* reverse: 5′-ACCTCCGGCTCCAGTACTTC-3′.
m*Nfil3/E4bp4* forward: 5′-GGAGCAGAACCACGATAACC-3′.
m*Nfil3/E4bp4* reverse: 5′-TTCCCCAGTCTTCTTTCAGG-3′.
m*Bmal1* forward: 5′-AACCTTCCCGCAGCTAACAG-3′.
m*Bmal1* reverse: 5′-AGTCCTCTTTGGGCCACCTT-3′.
m*Clock* forward: 5′-TATTTGCAGGCACCAACATC-3′.
m*Clock* reverse: 5′-TTGCGGAGGTGTAGACTGTG-3′.
m*Ddit3* forward: 5′-GGAGGTCTTCCTCAGATG-3′.
m*Ddit3* reverse: 5′-GGACGCAGGGTCAAGAGTAG-3′.
m*Slc2a2* forward: 5′-AACATGATCTTCACGGCTGTC -3′.
m*Slc2a2* reverse: 5′-AGATGGTGCAGAAAAACATGC -3′.
m*Ins1* forward: 5′-ACTGGAGCTGGGAGGAAGC -3′.
m*Ins1* reverse: 5′-GTCGAGGTGGGCCTTAGTTG -3′.
m*Ins2* forward: 5′-GCCCTAAGTGATCCGCTACAATC-3′.
m*Ins2* reverse: 5′-GCAGCACTGATCTACAATGCCAC -3′.
m*Rab37* forward: 5′-ATGGAGACCAGTGCCAAGAC -3′.
m*Rab37* reverse: 5′-AGTCTCGGATCTGGAAGCTG -3′.
m*Gapdh* forward: 5′-AGTATGACTCCACTCACGGCAA-3′.
m*Gapdh* reverse: 5′-TCTCGCTCCTGGAAGATGGT-3′.
m*Rev-erbα* forward: 5′-CCCTGGACTCCAATAACAACACA-3′.
m*Rev-erbα* reverse: 5′-GCCATTGGAGCTGTCACTGTAG-3′.
m*Cry1* forward: 5′- CAGCAGACTCACTCACTCAAGC-3′.
m*Cry1* reverse: 5′-GACACTCTGGGCATCCTCTTC -3′.
m*Cry2* forward: 5′-AAGCTGGGCCACTGGATAG-3′.
m*Cry2* reverse: 5′-TGCCTTTCTCCTCACTCTCG-3′.
m*Per1* forward: 5′-ACAGCAGCCACGGTTCTC-3′.
m*Per1* reverse: 5′-AGGATCTTGAACGCTGCTG-3′.
m*Per2* forward: 5′-GAGCTCCGAGAGGTTCATCC-3′.
m*Per2* reverse: 5′-TGCCTTTCTCCTCACTCTCG-3′.
m*Rab27a* forward: 5′-GCCAACGGGACAAACATAAG-3′.
m*Rab27a* reverse: 5′-AGCTGATCCGCAGAGGTATG-3′.
m*Rab27b* forward: 5′-CGCAGCTACAGGACAGAATG-3′.
m*Rab27b* reverse: 5′-TCCGGAACCTGTGTCTTCTC-3′.
m*Sirt1* forward: 5′-TTGACCTCCTCATTGTTATTGG-3′.
m*Sirt1* reverse: 5′-TGTAGATGAGGCAAAGGTTCC-3′.

m*Ucp2* forward: 5′-ACTGTGCCCTTACCATGCTC-3′.
m*Ucp2* reverse: 5′-ACTACGTTCCAGGATCCCAAG-3′.

2.6. Glucose Test

Glucose tolerance tests were performed on 12-week-old male mice fasted for 16 h. Glucose was given orally by gavage (2 g/kg) or intraperitoneally (1 g/kg) at 0 min. Insulin tolerance tests were performed on randomly fed male mice injected intraperitoneally with insulin (0.75 units/kg). Tail blood was collected at 0, 2, 15, 30, 60, 90, and 120 min, and blood glucose concentrations were determined using ANTSENCE II (Horiba Industry). Plasma insulin levels were measured by enzyme-linked immunosorbent assay (Morinaga). Insulin tolerance tests were performed on randomly fed male mice injected intraperitoneally with insulin (0.75 units/kg). Tail blood was collected at 0, 30, 60, 90 and 120 min.

2.7. Assay of Insulin Secretion From Isolated Islets

Pancreatic islets were obtained from WT, TG-C, and TG-D mice at 8 or 9 weeks of age by collagenase digestion, as described previously (Uchida et al., 2007). In brief, five size-matched islets were incubated in 500 μl of Krebs-Ringer solutions containing glucose, KCl, carbachol, or glibenclamide for 30 min. Insulin concentrations in supernatants of the isolated islets were measured by enzyme-linked immunosorbent assay (Morinaga).

2.8. Measurement of Cytoplasmic Ca^{2+} Concentration

Single β-cells were isolated from WT, TG-C, and TG-D mice at 8 or 9 weeks of age and plated onto coverslips. Cytoplasmic Ca^{2+} concentrations ($[Ca^{2+}]_i$) in β-cells were measured as previously reported (Yosida et al., 2014; Dezaki et al., 2011). Briefly, β-cells were super-fused with HEPES-added Krebs-Ringer bicarbonate buffer (HKRB) at 37 °C, and $[Ca^{2+}]_i$ was measured by dual-wavelength fura-2 microfluorometry with excitation at 340/380 nm and emission at 510 nm. Fluorescence ratio images were produced using an Aquacosmos system (Hamamatsu Photonics). Cells used for single-cell experiments fulfilled the morphological and physiological criteria for insulin-positive β-cells, including the diameter and responsiveness to glucose and KCl. Effects of KCl on $[Ca^{2+}]_I$ were investigated at the completion of recording.

2.9. Pancreatic Perfusion

Eight-week-old mice were fasted for 16 h and used in perfusion experiments, which were performed as described previously (Miki et al., 2005). Briefly, after anesthetization with sodium pentobarbital, the superior mesenteric and renal arteries were ligated, and the aorta was tied off just below the diaphragm. The perfusate was infused through a catheter placed in the abdominal aorta and collected from the portal vein. The perfusate was mixed with Krebs-Ringer bicarbonate HEPES (KRBH) buffer supplemented with 4.6% dextran and 0.25% bovine serum albumin and bubbled with a 95% O_2–5% CO_2 gas mixture. The flow rate of the perfusate was set at 1 ml/min. KRBH buffer containing 2.8 mM glucose was perfused for 15 min, following by KRBH buffer containing 16.7 mM glucose for 45 min. During the perfusion period, the mouse's body temperature was kept at 37 °C with normal saline.

2.10. Morphometric Analysis of β-cell Mass

Pancreata harvested from male mice at 24 weeks of age were dissected, weighed, fixed, paraffin embedded, and sectioned. Five sections from each mouse were immunostained for insulin. The β-cell area, defined as the insulin–positive cell area, was quantified using image analysis software (Image J). Total β-cell mass was then assessed by multiplying the ratio of the β-cell area to the total tissue area on the entire section by pancreatic weight, as described previously (Maier et al., 2010).

2.11. Pancreatic Insulin Content

The whole pancreas was dissected free of fat and other tissues immediately after the mice were killed. The pancreata were extracted employing the acid ethanol method (Ma et al., 2004).

2.12. Electron Microscopy

Tissue preparation and electron microscopy were performed as described previously (Akiyama et al., 2009). In brief, WT or TG-C mice at 8–9 weeks of age were anesthetized with sodium pentobarbital (65 mg/kg i.p.) and intracardially perfused with 2% glutaraldehyde (vol./vol.) and 4% paraformaldehyde (vol./vol.) in 0.1 mol/l phosphate buffer (pH 7.4) containing 0.2% picric acid (vol./vol.). Pancreatic sections (1 mm thick) were post-fixed with 1% OsO4 (wt/vol.), block-stained with 2% uranyl acetate (wt/vol.), dehydrated, infiltrated with propylene oxide, placed in a mixture of propylene oxide and epoxy resin (1:1), and finally flat-embedded on siliconized glass slides in Epoxy resin. Ultrathin sections were double stained with uranyl acetate and lead citrate, and then observed with a Hitachi H-7500 electron microscope (Hitachi High-Technologies) operating at 80 kV.

2.13. Immunofluorescence

Harvesting and processing of adult mouse pancreatic tissues were performed as previously described (Ohta et al., 2011). Antigen retrieval was performed on tissue sections before staining. Thereafter, sections were incubated overnight with the following primary antibodies: guinea pig anti-insulin (1:4000; Sigma) and mouse anti-glucagon (1:4000; Abcam). Coverslips were mounted in antifade solution containing DAPI (Vectashield, Vecta Laboratories). The antigens were visualized using the appropriate secondary antibody conjugated with Fluorescein FITC and cyanine Cy3 (1:200; Jackson ImmunoResearch Laboratories). All images were digitally acquired, without further processing. Digital images were compiled using a BZ Analyzer (Keyence).

2.14. ATP/ADP Ratio Measurement

The ATP/ADP assay was performed with a BioVision apoSENSOR kit, on 20 islets, ten minutes after the addition of 3 mM or 17 mM glucose. Supernatant insulin levels were measured by enzyme-linked immunosorbent assay (Morinaga). The basal ATP/ADP ratio was measured, using 40 islets immediately after isolation.

2.15. ChIP-sequencing

ChIP sequences were determined using a ChIP kit from Millipore. Briefly, freshly isolated pancreatic islets were pooled and treated with 1% formaldehyde to achieve cross-linking for 15 min at room temperature. After washing, the islets were dissolved in SDS lysis buffer containing a proteinase inhibitor cocktail followed by sonication to shear chromatin. Pre-cleared chromatin from 2000 islets isolated from TG-C mice was used for ChIP sample incubation with 5 μg of rabbit anti-E4BP4 (sc-28,203; Santa Cruz). After incubation, the immunoprecipitated chromatin DNA was harvested, cross-link reversed, and purified. Chromatin DNA samples were submitted to Takara Bio for sequence analysis processing using Illumina GAII. The mapped tags for each sample were converted to a browser extensible data (BED) file, detailing the genomic coordinate of each tag. Summary files in the BED format were used for viewing in the UCSC Genome Browser, and to generate screenshots.

2.16. ChIP Assay

The ChIP assay was performed according to the manufacturer's instructions (ChIP assay kit; Millipore) to detect recruitment of RNA polymerase II (positive control), DBP, and E4BP4 to the regulatory elements in mouse *Ins1*, *Ins2*, *Slc2a2*, and *Rab37* genes. ChIP was performed on DNA extracted from 2000 islets isolated from WT and TG-C mice. Normal rabbit IgG (sc-2027; Santa Cruz), rabbit anti-RNA polymerase II (Millipore), rabbit anti-DBP antibody (AVIVA SYSTEM BIOLOGY), and anti-E4BP4 (sc-28,203; Santa Cruz) were used for immunoprecipitation. PCR was performed for 38–40 cycles of 30 s each at 95 °C for the melting, 56 °C for the annealing, and 72 °C for the extension steps. An aliquot of the PCR product was fractionated on a 1.2% agarose gel containing ethidium bromide for UV visualization. The sequences of the primers were as follows:

m*Ins1* forward: 5′-TGCTCAGCCAAAGATGAAGA -3′.
m*Ins1* reverse: 5′-CTGCTTGCTGATGGTCTCTG -3′.
m*Ins2* forward: 5′-TGGCTCTCCTTGGGAACTTA -3′.
m*Ins2* reverse: 5′-TCTCATGGGGGAGAGAAATG -3′.
m*Slc2a2* forward: 5′-TGAAGCTTGGGGATCATTTC-3′.
m*Slc2a2* reverse: 5′-CCCAACAAGACCATCCTCTG-3′.
m*Rab37* forward: 5′-GTCAAGAGGGGGAAAATGCT-3′.
m*Rab37* reverse: 5′-CAGTCAGACCACTGCCGTTA-3′.

2.17. Microarray Analysis

Total cellular RNA was isolated from mice using ISOGEN (Nippon Gene) and the RNeasy Kit (Qiagen). Labeling and hybridization to the Affymetrix Mouse Genome 430 2.0 Array and the Affymetrix Mouse Gene 1.0 ST Array were performed at, respectively, KURABO (Osaka, Japan) and Bio Matrix Research (Chiba, Japan), following standard Affymetrix procedures.

2.18. Statistical Analysis

Statistical analyses were performed using Student's *t*-test or Welch's *t*-test to compare experimental groups with the control group. Data are presented as means ± SEM and differences were considered to be statistically significant at $p < 0.05$.

3. Results

3.1. Chronic ER Stress Attenuates DBP Transcriptional Activity Both In Vitro and In Vivo

To newly identify mechanisms underlying the dysfunction affecting β-cells in diabetic *Wfs1*$^{-/-}$ *A*^{y}/*a* mice, we performed microarray analyses and discovered a decrease in *Dbp* expression and an increase in *Nfil3*/*E4bp4* expression in *Wfs1*$^{-/-}$ *A*^{y}/*a* islets as compared to non-diabetic *A*^{y}/*a* islets (Akiyama et al., 2009; Nakabayashi et al., 2013). *Ddit3* expression was up-regulated in *Wfs1*$^{-/-}$ *A*^{y}/*a* islets as compared to *Ay*/*a* islets. No other clock genes, including *Arntl* (*Bmal1*), showed altered expressions (Supplementary Fig. 1a). Real-time RT-PCR was used to validate the microarray data. The Real time RT-PCR analysis of Wild type (WT), *A*^{y}/*a*, *Wfs1*$^{-/-}$, and *Wfs1*$^{-/-}$ *A*^{y}/*a* islets revealed that *Dbp* and *Nfil3*/*E4bp4* expression levels had decreased to one-third and increased about three-fold, respectively, in *Wfs1*$^{-/-}$ *A*^{y}/*a* as compared to WT islets (Fig. 1a). MIN6 cells treated with 1 μM thapsigargin (TG) for 24 h showed a marked decrease in *Dbp* mRNA and a marked increase in *Nfil3*/*E4bp4* mRNA. Meanwhile, *Ddit3* mRNA increased 24-fold as compared with the level in controls (Fig. 1b). Isolated islets treated with 0.5 μM TG for 24 h or 2 μg/ml tunicamycin (TM) showed very similar changes in the expressions of clock genes and *Ddit3* (Fig. 1c and d). MIN6 cells treated with TG and isolated islets treated with TG or TM showed increases in *Bmal1*, *Clock*, *Per* and *Cry* mRNAs, the exception being *Per3* mRNA (Fig. 1b–d and Supplementary Fig. 1b–d). The BMAL1 and CLOCK gene products, through interactions with E-box regulatory sites, activate many circadian rhythm genes, including PER and CRY. The PER:CRY complex translocates to the nucleus where it inhibits the BMAL1:CLOCK heterodimer. Based on our current observations, we were not able to determine whether ER stress increases or decreases E-box dependent transcriptional activity. MIN6 cells treated with 0.2 μg/ml H_2O_2 for 12 h showed no significant alterations in the expressions of clock genes including *Dbp* and *Nfil3*/*E4bp4* (data not shown). Overall, and most importantly, chronic ER stress clearly decreases DBP transcriptional activity in β-cells.

3.2. Transgenic Mice Expressing E4BP4 Under the Control of the Mouse Insulin I Gene Promoter Display Severely Impaired Insulin Secretion

To examine the role of DBP in β-cells, we generated transgenic mice expressing E4BP4 under the control of the highly β-cell specific mouse *insulin I* gene promoter (MIP) (Hara et al., 2006) (Supplementary Fig. 2a). We generated 2 lines of MIP-E4BP4 mice, TG-C and TG-D, which have 10 and 3 transgene copies, respectively (Supplementary Fig. 2b). Real-time RT-PCR confirmed 182- and 60-fold up-regulations of *Nfil3*/*E4bp4* mRNA in islets isolated from TG-C and TG-D mice at Zeitgeber time (ZT) 12, respectively, and these increases were associated with higher nuclear protein levels of E4BP4 (Fig. 2a and b).

Oral glucose tolerance tests (OGTT) revealed that both TG-C and TG-D mice displayed remarkable glucose intolerance with severely impaired insulin secretion. Glucose excursion in TG-C mice was higher than that in TG-D mice, indicating gene-dose dependent effects on the severity of these phenotypes (Fig. 2c–f). To evaluate insulin secretory capacity in vivo, we analyzed insulin secretion in the perfused pancreas. Perfusion with 17 mM glucose elicited substantial insulin secretion in WT mice. In contrast, TG-C and TG-D mice obviously had reduced and delayed insulin secretion during perfusion with 16.8 mM glucose (Fig. 2g and h).

The insulin secretory function of MIP-E4BP4 islets was also evaluated by means of static incubation. Glucose-stimulated insulin release in isolated islets was significantly reduced in TG-C and TG-D islets, whereas there were no significant differences in KCl-induced insulin secretion among the three groups. Insulin release stimulated by carbachol was significantly increased in TG-C and TG-D islets. Insulin release triggered by glibenclamide was significantly reduced in TG-C, but not in TG-D, islets (Fig. 2i).

MIP-E4BP4 mice were indistinguishable in body weight from control littermates (data not shown). Blood glucose concentrations were significantly higher in MIP-E4BP4 mice than in WT littermates, in the fed state, until 20 weeks of age (Supplementary Fig. 2c). Although plasma insulin concentrations in the fed state tended to be lower in TG-C mice than in WT littermates, the difference was not statistically significant (data not shown). Insulin tolerance tests revealed that TG-C mice were more insulin sensitive than WT, but not TG-D, mice (Supplementary Fig. 2d). These findings clearly show impaired insulin secretion to be the primary defect in MIP-E4BP4 mice.

3.3. An Increase in the Basal ATP/ADP Ratio in Islets Causes Impaired Insulin Secretion in MIP-E4BP4 Mice

To further investigate the mechanisms underlying β-cell dysfunction in MIP-E4BP4 islets, we studied the observed changes in the glucose-stimulated ATP/ADP ratio. While islets from WT mice displayed an approximately 1.8-fold glucose-induced increase in the ATP/ADP ratio, islets from TG-C mice lost all responsiveness, in association with reduced glucose-stimulated insulin secretion (Fig. 3a). Basal ATP/ADP ratios notably oscillated in a circadian manner in WT islets. Similar patterns were seen when comparing changes in the basal ATP/ADP ratio and changes in *Nfil3*/*E4bp4* mRNA expression in islets, suggesting that the basal ATP/ADP ratio oscillates in a phase opposite that of DBP transcriptional activity. In contrast, in TG-C islets, the basal ATP/ADP ratio

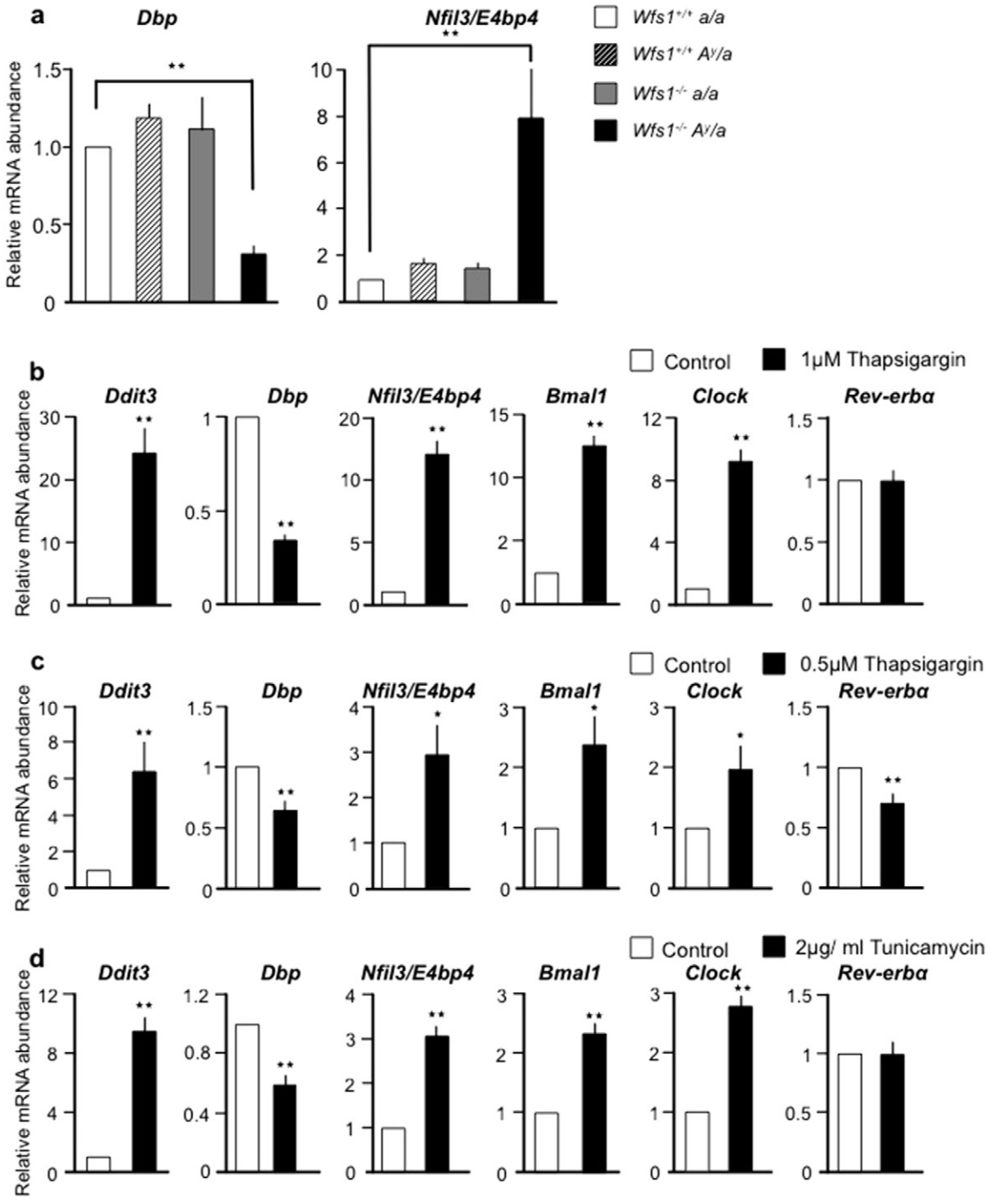

Fig. 1. Attenuation of DBP transcriptional activity induced by chronic ER stress. (a) The *Dbp* and *Nfil3/E4bp4* mRNA expression levels in *Wfs1*$^{+/+}$ *a/a*, *Wfs1*$^{+/+}$ *A*^{y}*/a*, *Wfs1*$^{-/-}$ *a/a* and *Wfs1*$^{-/-}$ *A*^{y}*/a* islets at ZT12. Data are presented as relative expressions, and each point represents the mean + SEM (N = 3/group; **p < 0.01). (b–c) MIN6 cells (b) and mouse islets (c) were incubated with thapsigargin at the indicated concentrations for 24 h and then subjected to real-time RT-PCR. Data are expressed relative to the values for cells incubated without thapsigargin and are the means + SEM of six experiments. *p < 0.05, **p < 0.01. (d) Mouse islets were incubated with tunicamycin at the indicated concentrations for 24 h and then subjected to real-time RT-PCR. Data are expressed relative to the values for cells incubated without tunicamycin and are the means + SEM of six experiments. **p < 0.01.

is markedly elevated and the oscillation pattern is altered in accordance with changes in the E4BP4 expression level and oscillation (Fig. 3b). Basal ATP/ADP ratios were found to be higher in TG-D and *Wfs1*$^{-/-}$ *A*^{y}*/a* islets than in WT islets (Fig. 3c). Our results suggest that mitochondrial respiration has been altered and glucose-stimulated insulin release could, at least in part, be inhibited by high basal ATP/ADP ratios in MIP-E4BP4 and *Wfs1*$^{-/-}$ *A*^{y}*/a* islets. In support of this notion, the Ca^{2+} responses to glucose in β-cells from MIP-E4BP4 mice were also significantly attenuated as compared with those observed in WT mice. The Ca^{2+} response to KCl was intact (Fig. 3d–g). These results indicate the important role of DBP and E4BP4 in insulin secretion affecting intracellular metabolism, the ATP/ADP ratio, and the Ca^{2+} response to glucose.

Accumulating evidence indicates that NAD^{+}-dependent deacetylase sirtuin 1 (SIRT1) plays critical roles in regulating insulin secretion (Moynihan et al., 2005; Bordone et al., 2006; Luu et al., 2013). In TG-C islets, the expression of *Sirt1* was decreased at ZT8 and the expression of mitochondrial uncoupling protein 2 (*Ucp2*) was increased at ZT0 and ZT20, exhibiting modest circadian oscillations (Supplementary Fig. 3a). In previous studies, it was suggested that SIRT1 exerts beneficial effects on insulin secretion by suppressing UCP2 expression and that a

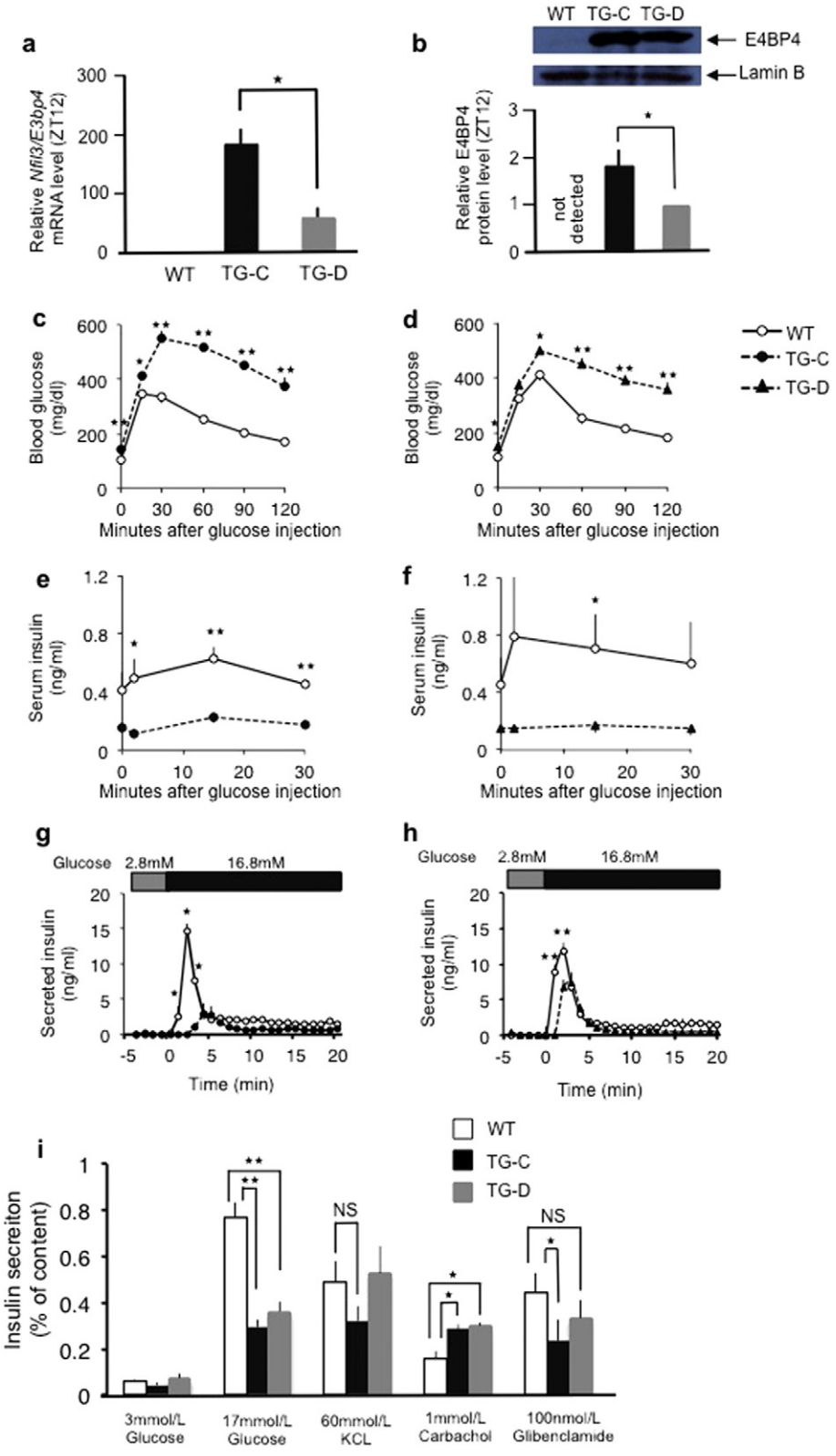

Fig. 2. Impaired glucose tolerance and defective insulin secretion in MIP-E4BP4 mice. (a) The *Nfil3/E4bp4* mRNA expression levels in islets of 8-week-old WT (N = 6), TG-C (N = 7), and TG-D (N = 6) mice at ZT12. Data are means + SEM relative to the value of WT mice. ⋆p < 0.05. (b) Immunoblot analysis of E4BP4 in islets isolated from 8-week-old WT (N = 3), TG-C (N = 4), and TG-D (N = 4) mice at ZT12. Data are means + SEM relative to the value of TG-D mice. ⋆p < 0.05. (c–d) Blood glucose concentrations of TG-C (WT N = 9; TG-C N = 8) (c) and TG-D (WT N = 6; TG-D N = 7) (c) mice during OGTT. Data are means ± SEM. ⋆p < 0.05, ⋆⋆p < 0.01. (e–f) Serum insulin levels of TG-C (WT N = 9; TG-C N = 8) (e) and TG-D (WT N = 6; TG-D N = 7) (F) mice during OGTT. Data are means ± SEM. ⋆p < 0.05, ⋆⋆p < 0.01. (g–h) Insulin secretion during pancreatic perfusion. Effects of a glucose increase on insulin secretion from the perfused pancreases of TG-C (g) (WT n = 3; TG-C n = 5) and TG-D (h) (WT n = 5; TG-D n = 4) mice are shown. Data are means ± SEM. ⋆p < 0.05, ⋆⋆p < 0.01. (i) Insulin secretion in batch-incubated pancreatic islets isolated from WT (open bars), TG-C (solid bars), and TG-D (gray bars) mice at 8 or 9 weeks of age. Data are means + SEM from at least 6 experiments. NS, non-significant, ⋆p < 0.05, ⋆⋆p < 0.01 (WT versus TG-C or TG-D).

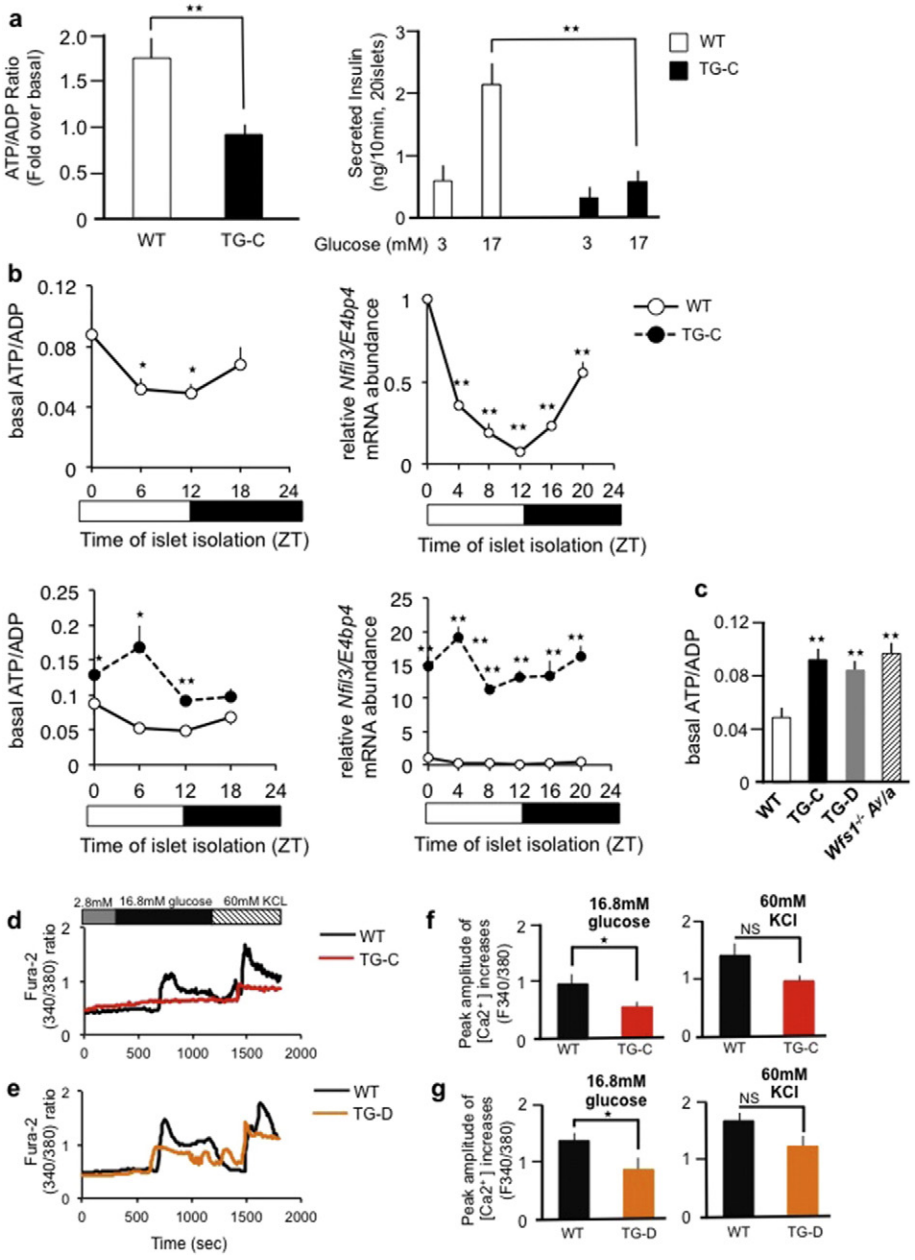

Fig. 3. An increase in the basal ATP/ADP ratio in islets causes impaired insulin secretion in MIP-E4BP4 mice. (a) Fold change over the basal ATP/ADP ratio and simultaneously measured insulin release in islets isolated from WT and TG-C mice at ZT12 after exposure to 3 and 17 mM glucose concentrations. Data are means + SEM (N = 5/per group; $^{**}p < 0.01$). (b) The basal ATP/ADP ratios in isolated islets during a 12 h light-dark cycle (at least four mice per time point) and real-time RT-PCR analysis of *Nfil3/E4bp4* in isolated islets during this 12 h light-dark cycle (n = 6 per time point). Data are means ± SEM. $^{*}p < 0.05$, $^{**}p < 0.01$ (left panel, ZT0 versus indicated time point; right panel, WT versus TG-C). (c) The basal ATP/ADP ratios in islets isolated at ZT12 from WT (N = 10), TG-C (N = 6), TG-D (N = 4), and *Wfs1*$^{-/-}$ *A*^{y}*/a* (N = 4) mice. Data are means + SEM. $^{**}p < 0.01$ (WT versus TG-C, TG-D, or *Wfs1*$^{-/-}$ *A*^{y}*/a*). (d–e) Typical time courses showing intracellular Ca^{2+} during application of 16.8 mM glucose or 60 mM KCl in β-cells isolated from TG-C (d) or TG-D (e) islets. (f–g) Peak amplitudes induced by 16.8 mM glucose (left panels) or 60 mM KCl (right panels) in β-cells isolated from TG-C (WT N = 4; TG-C N = 3) (f) or TG-D (WT N = 5; TG-D N = 5) (g) mice. Data are means + SEM. NS, non-significant, $^{*}p < 0.05$.

decrease in β-cell SIRT1 expression impaired insulin secretion (Moynihan et al., 2005). Damage to the SIRT1-UCP2 pathway might be partially responsible for changes in the ATP/ADP ratio, and thereby account for the impaired glucose stimulated insulin secretion in TG-C mice.

3.4. DBP and E4BP4 Directly Regulate the Transcription of Genes Linked to Insulin Secretion in a Circadian Manner

TG-C islets showed significantly increased expression of *Dbp* RNA only at ZT8 and *Bmal1* mRNA only at ZT4. TG-C islets tended to show increased expressions of *Clock* gene mRNAs during the daytime (Fig. 4a). The rhythms of *Per1*, *Per2 and Rev.-erbα* expressions in TG-C islets were almost the same as those in WT islets, though the oscillation amplitudes of these gene expressions tended to be attenuated in TG-C islets (Supplementary Fig. 3a).

In WT islets, mRNA expressions of genes involved in insulin secretion (*Slc2a2*, *Ins1*, *Ins2*, and *Rab37*) (Ljubicic et al., 2013) exhibited circadian oscillation. Starting around the beginning of the feeding period, they gradually increased. This circadian oscillation was severely impaired in the TG-C islets (Fig. 4a). Similarly, the amplitude of *Rab27a* (Wang et al., 2013), which displayed circadian rhythmicity similar to

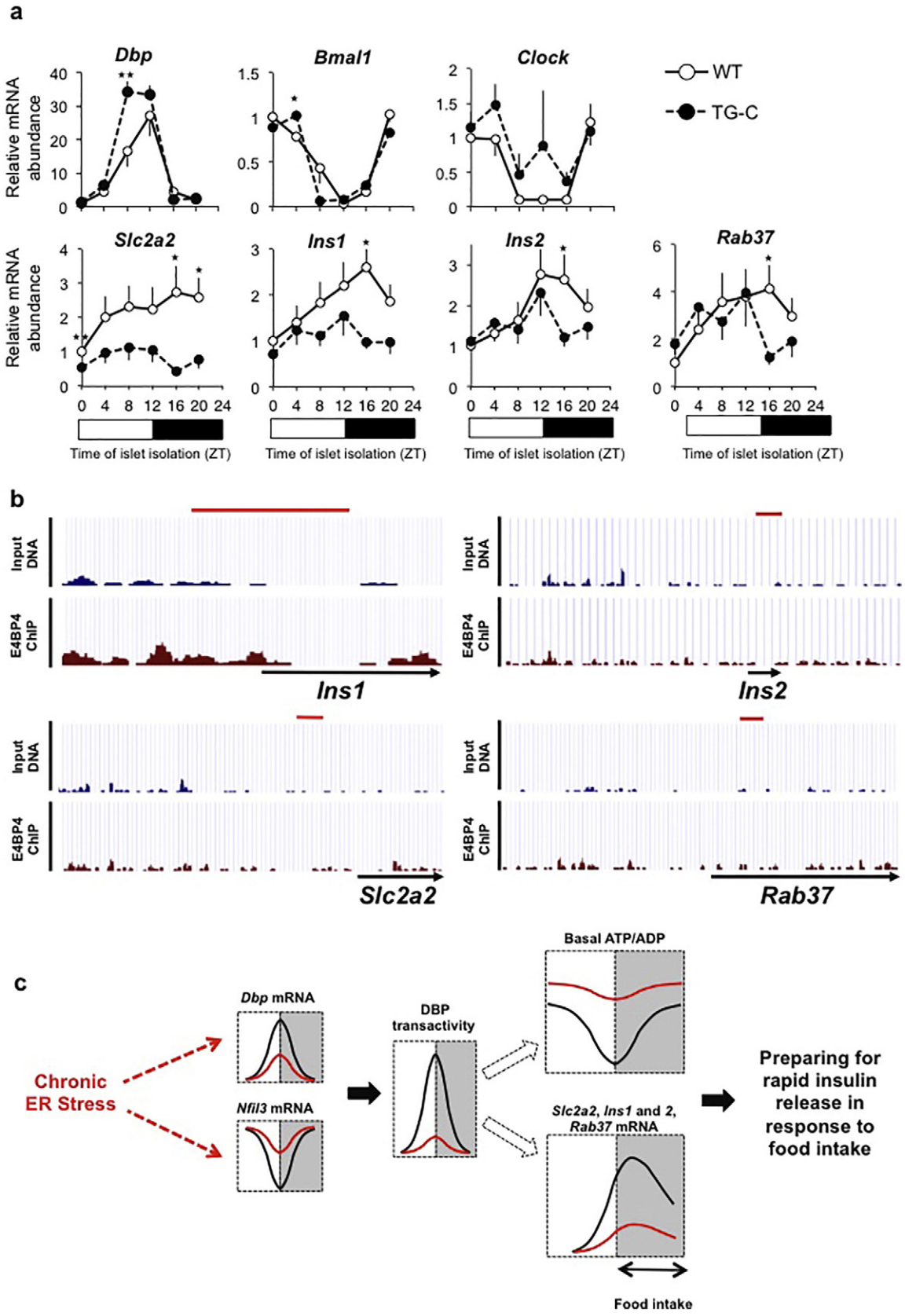

Fig. 4. DBP and E4BP4 directly regulate the transcription of genes linked to insulin secretion. (a) Real-time PCR analysis of clock-controlled genes, *Slc2a2*, *Ins1*, *Ins2* and *Rab37*, in isolated islets during a 12 h light-dark cycle (N = 6 per time point). Data are means ± SEM. *p < 0.05, **p < 0.01 (controls versus TG-C). (b) E4BP4 at the selected gene promoters in pancreatic islets isolated from TG-C mice. UCSC genome browser images of E4BP4 profiles at *Ins1*, *Ins2*, *Slc2a2* and *Rab37* in TG-C mice. Chromosome coordinates are indicated at the top. The plot in the middle shows the density of ChIP-seq reads with the peak score indicated on the Y-axis. The *Ins1*, *Ins2*, *Slc2a2* and *Rab37* genes are shown at the bottom. Red scale bars indicate 1 kb of genome. (c) Schematic models depicting the circadian control of insulin release via regulation of the basal ATP/ADP ratio and the gene expressions of *Slc2a2*, *Ins1*, *Ins2* and *Rab37* in islets.

that of *Rab37*, tended to be attenuated in TG-C islets (Supplementary Fig. 3a). Microarray analysis of islets isolated at ZT8 revealed only the *Slc2a2* RNA level to be reduced among the genes directly involved in insulin secretion in TG-C mice (Supplementary Table 1). We further investigated, by employing E4BP4 chromatin immunoprecipitation sequencing (ChIP-seq) using TG-C islets, whether E4BP4 overexpression directly affects the gene expressions involved in insulin secretion (*Ins1*, *Ins2*, *Slc2a2,* and *Rab37*). Obvious E4BP4 enrichment in the *Ins1* promoter region and slight enrichment in the *Ins2*, *Slc2a2*, and *Rab37* promoter regions was observed, suggesting that DBP and E4BP4 directly regulate, at least to some degree, the expressions of genes involved in insulin secretion (Fig. 4b). ChIP-PCR analysis of isolated islets from WT and TG-C mice showed that over-expressed E4BP4 significantly competed with DBP for binding to the regulatory regions of *Ins1* and *Ins2* (Supplementary Fig. 3b and c). Although not significant, similar trends were observed in *Slc2a2* and *Rab37* (Supplementary Fig. 3b and c).

3.5. Decreased Insulin Content and Abnormal Islet Morphology in TG-C Mice

Pancreatic insulin content and β-cell mass were decreased in TG-C islets, but not in TG-D islets (Supplementary Fig. 2e and f), and this alteration was associated with a smaller number of insulin granules (Supplementary Fig. 2g), especially those located within 0.15 μm of the plasma membrane (PM) (data not shown). Differences in islet structure were obvious in TG-C mice at 24 weeks of age (Supplementary Fig. 2h). The ratio of β- to α-cells was significantly decreased (Supplementary Fig. 2i), while the proportion of islets with α-cells in the center was clearly increased, in TG-C mice (Supplementary Fig. 2j). Impaired insulin release might, at least to some extent, be associated with the observed changes in islet morphology and the reduced insulin content of TG-C islets.

3.6. High Fat-diet Exerted a Gene-dosage-dependent Effect on β-cell Failure in MIP-Nfil3/E4BP4 Mice

We further investigated the effects of high fat (HF)-diet-induced insulin resistance on E4BP4 transgenic mice. Four-week-old MIP-E4BP4 and WT mice were fed a HF-diet for 8 weeks. MIP-E4BP4-HF mice showed severely impaired glucose tolerance as compared to WT-HF mice with marked impairment of insulin secretion (Supplementary Fig. 4a). MIP-E4BP4-HF mice also had significantly higher non-fasting glucose levels and tended to have lower insulin levels than WT mice (Supplementary Fig. 4b). Pancreatic insulin content in TG-C-HF mice was decreased by approximately 75% as compared to that in the HF-diet fed WT mice (Supplementary Fig. 4c). Similar findings were obtained in TG-D-HF mice, although the difference did not reach statistical significance (Supplementary Fig. 4c). The gene-dose effect was more prominent with HF-diet feeding.

3.7. DBP Transcriptional Activity Contributes to the Circadian Difference in Insulin Secretion in Mice

Glucose-stimulated insulin secretion is reportedly higher in the morning than in the afternoon in humans (Sonnier et al., 2014). To investigate the relationship between DBP transcriptional activity and insulin secretion in WT mice, oral glucose tolerance tests (OGTT) were performed at ZT1 and at ZT13. The serum insulin response 2 min after a glucose load, expressed as a percentage of the initial insulin level, was significantly lower at ZT1 than at ZT13. Plasma glucose excursion showed a difference at 30 min. These observations suggest a relationship between DBP transcriptional activity and insulin secretion (Supplementary Fig. 4d).

4. Discussion

Our results clearly demonstrate the pivotal roles of DBP and E4BP4 transcriptional activity in the regulation of insulin secretion, in connection with circadian regulation, and in ER stress responses.

The UPR is an essential component of β-cell protection from ER stress. Interestingly, a circadian disruption, induced by phase advancement, accelerated β-cell loss in diabetes-prone human islet amyloid polypeptide transgenic rats, that are known to have ER stress (Gale et al., 2011). The study by Gale and colleagues showed sleep deprivation in mice to lead to ER stress affecting the entire pancreas, supporting the notion that circadian disruption may worsen unresolved ER stress, thereby producing β-cell dysfunction. On the other hand, our own observations suggest that circadian clock genes, especially DBP and E4BP4, are regulated by ER stress in the context of β-cell failure (Fig. 4c). Thus, the circadian-ER stress connection might be bidirectional and have significant implications for β-cell dysfunction. MIN6 cells treated with TG and isolated islets treated with TG or TM showed increases in *Bmal1*, *Clock*, *Per* and *Cry* mRNAs, the exception being *Per3* mRNA (Fig. 1b–d and Supplementary Fig. 1b–d). However, whether ER stress influences E-box dependent transcriptional activity remains unclear. *Dbp* regulatory region has an E-box element. Therefore increase of BMALl1 and CLOCK should basically increase *Dbp* expression. According to our observations, however, ER stress probably suppresses *Dbp* expression without interaction of BMAL1 and CLOCK.

Surprisingly, in MIP-E4BP4 islets, the expression levels of *Bmal1*, *Clock*, *Per1*, *Per2*, *Dbp*, and *Rev.-erbα* mRNA were not reduced at any of the time points examined (Fig. 4a and Supplementary Fig. 3a). *Clock* mutant and β-cell specific *Bmal1* deficient mice showed complete disruption of rhythmic *Dbp* expression in islets (Marcheva et al., 2010; Perelis et al., 2015). In addition, MIP-E4BP4 mice have a more distinct phenotype than *Clock* mutant and β-cell specific *Bmal1* deficient mice (Marcheva et al., 2010; Perelis et al., 2015). These observations support the premise that DBP and E4BP4 play a role in the pathway leading to β-cell failure following circadian misalignment (Fig. 4c).

The mechanism whereby circadian misalignment in β-cells causes β-cell failure has not been fully elucidated. However, at least two components exist, i.e. secretory machinery defects and metabolic abnormalities. Expressions of key molecules involved in insulin secretion and regulation, such as *Slc2a2* (Glut2) and *Rab37*, as well as insulin genes were altered (Fig. 4a), along with islet morphology/β-cell number (Supplementary Fig. 2e–i). In addition, circadian rhythmicity of the cellular ATP/ADP ratio was disrupted, with constitutive elevation of the basal level, and the glucose-stimulated response was impaired (Fig. 4a and b). It is well known that the ATP/ADP ratio is a critical signal connecting glucose metabolism and insulin secretion in β-cells.

SIRT1 is well known to play a central role in the interplay between the circadian clock and metabolism. In addition, in previous studies, SIRT1 was also suggested to have beneficial effects on insulin secretion and a decrease in β-cell SIRT1 expression was found to impair insulin secretion by disrupting glucose sensing (Luu et al., 2013; Moynihan et al., 2005). SIRT1 suppresses *Ucp2* transcription by direct binding to the *Ucp2* promoter (Bordone et al., 2006). While some studies have linked *Sirt1* knockdown to increased *Ucp2* (Moynihan et al., 2005; Bordone et al., 2006), β-cell specific *Sirt1* deficient mice showed no difference in *Ucp2* transcript levels as compared with controls (Luu et al., 2013). In TG-C islets, overall expression of *Sirt1* was decreased, and the expression of *Ucp2* was increased (Supplementary Fig. 3a). Our findings, along with those of previous studies, suggest limited positive associations among DBP transactivity, the SIRT1-UCP2 axis, and glucose-stimulated insulin secretion depending on the expression levels of *Sirt1* and *Ucp2*, although this speculation needs to be experimentally tested.

Basically, circadian rhythms are recurrent patterns in numerous physiological processes that have been documented even in plants and cyanobacteria, in addition to animals, within a period of one day. The ATP/ADP ratios in cyanobacterial cells and sunflower roots are

actually higher in the dark than in the light and oscillate in a circadian manner (Pattanayak et al., 2014; Knight and Weissman, 1982). In mouse islets, the basal ATP/ADP ratio exhibits circadian oscillation associated with overall DBP activity (Fig. 3b). Furthermore, a constitutive reduction in DBP activity abolished normal oscillation of the ATP/ADP ratio, with sustained ATP/ADP elevation (Fig. 3b). Chronically exposing rat pancreatic islets to leucine reduces glucose-stimulated insulin release associated with an increased basal ATP/ADP ratio in the presence of a basal (2.8 mM) glucose concentration (Anello et al., 2001). Taking these observations into consideration, loss of circadian rhythmicity and a constitutively elevated basal ATP/ADP ratio might contribute to the impaired glucose-stimulated insulin secretion in MIP-E4BP4 and *Wfs1*$^{-/-}$ *A*^{y}/*a* mice.

There is a major difference between diurnal and nocturnal insulin secretion in normal mice (Supplementary Fig. 4d), and also in humans (Sonnier et al., 2014). In the circadian cycle, DBP transactivity is expected to be the strongest around the beginning of the active time of day (mice: nighttime, humans: daytime). In general, an hour or so before we awaken, body temperature increases, the gastrointestinal tract starts moving again, and cellular metabolism accelerates to provide energy to support the day's activities. Digestion/absorption systems also prepare for the ingestion of breakfast based on the local time. At the same time, pancreatic β-cells probably prepare to secrete insulin. Our findings suggest that DBP transcriptional activity is an essential component of preparing β-cells to release insulin (Fig. 4c).

HF-diet feeding induces obesity and increases the risk of developing metabolic disorders. However, time-restricted feeding of a HF-diet without caloric reduction suppresses obesity and other metabolic diseases (Hatori et al., 2012). Recently, time-restricted feeding was shown to be effective for stabilizing and reversing the progression of metabolic diseases including T2DM in mice (Chaix et al., 2014). These remarkable effects of time-restricted feeding are probably due to fine-tuning of circadian clocks. Our results suggest fine-tuning of DBP to be absolutely critical for preventing metabolic diseases, especially in terms of appropriate insulin responsiveness by pancreatic β-cells. Feeding during the bathyphase of DBP transcriptional activity may underlie, or at least contribute to, the metabolic dysfunctions observed in subjects with a shiftwork schedule.

The primary defect in diabetes of Wolfram syndrome patients and WFS1 deficient mice is insulin secretory failure. Both humans and mice deficient in WFS1 have selective β-cell loss, possibly associated with chronically elevated β-cell ER stress and dysregulated ER stress responses (Karasik et al., 1989; Riggs et al., 2005). β-cell functional abnormalities also include canonical impairment of glucose stimulated insulin secretion (Hatanaka et al., 2011). It is well known that β-cell ER stress is also involved in β-cell failure in common T2DM associated with glucoliptoxicity and other mechanisms. In addition, variations in the *WFS1* gene are also shown to predispose a person to T2DM (Sandhu et al., 2007). Therefore, although our findings are mostly from animal models and with limitations, they would be relevant to humans. Modulation of clock genes could be therapeutic strategies and greatly improve treatment of Wolfram syndrome-associated diabetes and common T2DM.

Conflict of Interest

There are no conflicts of interest to this study.

Author Contributions

Y.O., A.T., T.M., H.N., M.A., R.S., R.F., K.Y., and A.Y. performed the experiments. Y.O., A.T., and Y.T. designed the experiments and interpreted the data. Y.O., A.T., A.Y., K.S., and Y.T. reviewed and edited the manuscript. Y.O., A.T., and Y.T. developed the project and wrote the manuscript. Y.T. coordinated and directed the project. All authors approved the final version of the manuscript.

Funding Sources

This research was supported by grants, from the Japan Society for the Promotion of Science, 26460489 (to Y.O.) and 23390080 and 15H04849 (to Y.T.), as well as a grant from Takeda Science Foundation.

Acknowledgements

We thank Y. Kosaka, N. Kishimoto, and M. German at the UCSF Diabetes Center for assistance with obtaining the MIP-EGFP construct. We are grateful for the technical contributions of M. Tamaki, Y. Fujitani, and H. Watada at Juntendo University. We are also grateful for the technical contribution of K. Dezaki at the Jichi University School of Medicine. We thank Prof. J. Bass at Northwestern University for helpful discussions.

Appendix A. Supplementary data

Supplementary data to this article can be found online at http://dx.doi.org/10.1016/j.ebiom.2017.03.040.

References

Akiyama, M., Hatanaka, M., Ohta, Y., Ueda, K., Yanai, A., Uehara, Y., Tanabe, K., Tsuru, M., Miyazaki, M., Saeki, S., et al., 2009. Increased insulin demand promotes while pioglitazone prevents pancreatic beta cell apoptosis in Wfs1 knockout mice. Diabetologia 52, 653–663.

Anello, M., Ucciardello, V., Piro, S., Patané, G., Frittitta, L., Calabrese, V., Giuffrida Stella, A.M., Vigneri, R., Purrello, F., Rabuazzo, A.M., 2001. Chronic exposure to high leucine impairs glucose-induced insulin release by lowering the ATP-to-ADP ratio. Am. J. Physiol. Endocrinol. Metab. 281, E1082–E1087.

Bachar, E., Ariav, Y., Ketzinel-Gilad, M., Cerasi, E., Kaiser, N., Leibowitz, G., 2009. Glucose amplifies fatty acid-induced endoplasmic reticulum stress in pancreatic beta-cells via activation of mTORC1. PLoS One 4, e4954.

Bordone, L., Motta, M.C., Picard, F., Robinson, A., Jhala, U.S., Apfeld, J., McDonagh, T., Lemieux, M., McBurney, M., Szilvasi, A., Easlon, E.J., Lin, S.J., Guarente, L., 2006. Sirt1 regulates insulin secretion by repressing UCP2 in pancreatic beta cells. PLoS Biol. 4, e31.

Chaix, A., Zarrinpar, A., Miu, P., Panda, S., 2014. Time-restricted feeding is a preventative and therapeutic intervention against diverse nutritional challenges. Cell Metab. 20, 991–1005.

Cirelli, C., Tononi, G., 2004. Uncoupling proteins and sleep deprivation. Arch. Ital. Biol. 142, 541–549.

Cornelis, M.C., Fu, F.B., 2012. Gene-environment interactions in the development of type 2 diabetes: recent progress and continuing challenges. Annu. Rev. Nutr. 32, 245–259.

Delépine, M., Nicolino, M., Barrett, T., Golamaully, M., Lathrop, G.M., Julier, C., 2000. EIF2AK3, encoding translation initiation factor 2-alpha kinase 3, is mutated in patients with Wolcott-Rallison syndrome. Nat. Genet. 25, 406–409.

Dezaki, K., Damdindorj, B., Sone, H., Dyachok, O., Tengholm, A., Gylfe, E., Kurashina, T., Yoshida, M., Kakei, M., Yada, T., 2011. Ghrelin attenuates cAMP-PKA signaling to evoke insulinostatic cascade in islet β-cells. Diabetes 60, 2315–2324.

Fonseca, S.G., Fukuma, M., Lipson, K.L., Nguyen, L.X., Allen, J.R., Oka, Y., Urano, F., 2005. WFS1 is a novel component of the unfolded protein response and maintains homeostasis of the endoplasmic reticulum in pancreatic beta-cells. J. Biol. Chem. 280, 39609–39615.

Gale, J.E., Cox, H.I., Qian, J., Block, G.D., Colwell, C.S., Matveyenko, A.V., 2011. Disruption of circadian rhythms accelerates development of diabetes through pancreatic beta-cell loss and dysfunction. J. Biol. Rhythm. 26, 423–433.

Hara, M., Dizon, R.F., Glick, B.S., Lee, C.S., Kaestner, K.H., Piston, D.W., Bindokas, V.P., 2006. Imaging pancreatic beta-cells in the intact pancreas. Am. J. Physiol. Endocrinol. Metab. 290, E1041–E1047.

Harding, H.P., Zhang, Y., Bertolotti, A., Zeng, H., Ron, D., 2000. Perk is essential for translational regulation and cell survival during the unfolded protein response. Mol. Cell 5, 897–904.

Hatanaka, M., Tanabe, K., Yanai, A., Ohta, Y., Kondo, M., Akiyama, M., Shinoda, K., Oka, Y., Tanizawa, Y., 2011. Wolfram syndrome 1 gene (WFS1) product localizes to secretory granules and determines granule acidification in pancreatic beta-cells. Hum. Mol. Genet. 20, 1274–1284.

Hatori, M., Vollmers, C., Zarrinpar, A., DiTacchio, L., Bushong, E.A., Gill, S., Leblanc, M., Chaix, A., Joens, M., Fitzpatrick, J.A., Ellisman, M.H., Panda, S., 2012. Time-restricted feeding without reducing caloric intake prevents metabolic diseases in mice fed a high-fat diet. Cell Metab. 15, 848–860.

Inoue, H., Tanizawa, Y., Wasson, J., Behn, P., Kalidas, K., Bernal-Mizrachi, E., Mueckler, M., Marshall, H., Donis-Keller, H., Crock, P., et al., 1998. A gene encoding a transmembrane protein is mutated in patients with diabetes mellitus and optic atrophy (Wolfram syndrome). Nat. Genet. 20, 143–148.

Karasik, A., O'Hara, C., Srikanta, S., Swift, M., Soeldner, J.S., Kahn, C.R., Herskowitz, R.D., 1989. Genetically programmed selective islet beta-cell loss in diabetic subjects with Wolfram's syndrome. Diabetes Care 12, 135–138.

Knight, T.J., Weissman, G.S., 1982. Rhythms in glutamine synthetase activity, energy charge, and glutamine in sunflower roots. Plant Physiol. 70, 1683–1688.
Ljubicic, S., Bezzi, P., Brajkovic, S., Nesca, V., Guay, C., Ohbayashi, N., Fukuda, M., Abderrhamani, A., Regazzi, R., 2013. The GTPase Rab37 participates in the control of insulin exocytosis. PLoS One 8, e68255.
Luu, L., Dai, F.F., Prentice, K.J., Huang, X., Hardy, A.B., Hansen, J.B., Liu, Y., Joseph, J.W., Wheeler, M.B., 2013. The loss of Sirt1 in mouse pancreatic beta cells impairs insulin secretion by disrupting glucose sensing. Diabetologia 56, 2010–2020.
Ma, D., Shield, J.P., Dean, W., Leclerc, I., Knauf, C., Ré Burcelin, R., Rutter, G.A., Kelsey, G., 2004. Impaired glucose homeostasis in transgenic mice expressing the human transient neonatal diabetes mellitus locus, TNDM. J. Clin. Invest. 114, 339–348.
Mackiewicz, M., Shockley, K.R., Romer, M.A., Galante, R.J., Zimmerman, J.E., Naidoo, N., Baldwin, D.A., Jensen, S.T., Churchill, G.A., Pack, A.I., 2007. Macromolecule biosynthesis—a key function of sleep. Physiol. Genomics 31, 441–457.
Maier, B., Ogihara, T., Trace, A.P., Tersey, S.A., Robbins, R.D., Chakrabarti, S.K., Nunemaker, C.S., Stull, N.D., Taylor, C.A., Thompson, J.E., et al., 2010. The unique hypusine modification of eIF5A promotes islet beta cell inflammation and dysfunction in mice. J. Clin. Invest. 120, 2156–2170.
Marcheva, B., Ramsey, K.M., Buhr, E.D., Kobayashi, Y., Su, H., Ko, C.H., Ivanova, G., Omura, C., Mo, S., Vitaterna, M.H., et al., 2010. Disruption of the CLOCK components CLOCK and BMAL1 leads to hypoinsulinaemia and diabetes. Nature 466, 627–631.
Miki, T., Minami, K., Shinozaki, H., Matsumura, K., Saraya, A., Ikeda, H., Yamada, Y., Holst, J.J., Seino, S., 2005. Distinct effects of glucose-dependent insulinotropic polypeptide and glucagon-like peptide-1 on insulin secretion and gut motility. Diabetes 54, 1056–1063.
Moynihan, K.A., Grimm, A.A., Plueger, M.M., Bernal-Mizrachi, E., Ford, E., Cras-Méneur, C., Permutt, M.A., Imai, S., 2005. Increased dosage of mammalian Sir2 in pancreatic beta cells enhances glucose-stimulated insulin secretion in mice. Cell Metab. 2, 105–117.
Nakabayashi, H., Ohta, Y., Yamamoto, M., Susuki, Y., Taguchi, A., Tanabe, K., Kondo, M., Hatanaka, M., Nagao, Y., Tanizawa, Y., 2013. Clock-controlled output gene Dbp is a regulator of Arnt/Hif-1β gene expression in pancreatic islet β-cells. Biochem. Biophys. Res. Commun. 434, 370–375.
Nilsson, P.M., Rööst, M., Engström, G., Hedblad, B., Berglund, G., 2004. Incidence of diabetes in middle-aged men is related to sleep disturbances. Diabetes Care 27, 2464–2469.
Ohta, Y., Kosaka, K., Kishimoto, N., Wang, J., Smith, S.B., Honig, G., Kim, H., Gasa, R.M., Neubauer, N., Liou, A., et al., 2011. Convergence of the insulin and serotonin programs in the pancreatic β-cell. Diabetes 60, 3208–3216.
Pan, A., Schernhammer, E.S., Sun, Q., Hu, F.B., 2011. Rotating night shift work and risk of type 2 diabetes: two prospective cohort studies in women. PLoS Med. 8, e1001141.
Pattanayak, G.K., Phong, C., Rust, M.J., 2014. Rhythms in energy storage control the ability of the cyanobacterial circadian clock to reset. Curr. Biol. 24, 1934–1938.
Perelis, M., Marcheva, B., Ramsey, K.M., Schipma, M.J., Hutchison, A.L., Taguchi, A., Peek, C.B., Hong, H., Huang, W., Omura, C., et al., 2015. Pancreatic β cell enhancers regulate rhythmic transcription of genes controlling insulin secretion. Science 350, aac4250.
Pretty, M., Nolan, C.J., 2006. Islet beta cell failure in type 2 diabetes. J. Clin. Invest. 116, 1802–1812.
Qian, J., Block, G.D., Colwell, C.S., Matveyenko, A.V., 2013. Consequences of exposure to light at night on the pancreatic islet circadian clock and function in rats. Diabetes 62, 3469–3478.
Rakshit, K., Hsu, T.W., Matveyenko, A.V., 2016. Bmal1 is required for beta cell compensatory expansion, survival and metabolic adaptation to diet-induced obesity in mice. Diabetologia 59, 734–743.
Riggs, A.C., Bernal-Mizrachi, E., Ohsugi, M., Wasson, J., Fatrai, S., Welling, C., Murray, J., Schmidt, R.E., Herrera, P.L., Permutt, M.A., 2005. Mice conditionally lacking the Wolfram gene in pancreatic islet beta cells exhibit diabetes as a result of enhanced endoplasmic reticulum stress and apoptosis. Diabetologia 48, 2313–2321.
Sandhu, M.S., Weedon, M.N., Fawcett, K.A., Wasson, J., Debenham, S.L., Daly, A., Lango, H., Frayling, T.M., Neumann, R.J., Sherva, R., et al., 2007. Common variants in WFS1 confer risk of type 2 diabetes. Nat. Genet. 39, 951–953.
Sonnier, T., Rood, J., Gimble, J.M., Peterson, C.M., 2014. Glycemic control is impaired in the evening in prediabetes through multiple diurnal rhythms. J. Diabetes Complicat. 28, 836–843.
Uchida, T., Iwashita, N., Ohara-Imaizumi, M., Ogihara, T., Nagai, S., Choi, J.B., Tamura, Y., Tada, N., Kawamori, R., Nakayama, K.I., et al., 2007. Protein kinase Cdelta plays a non-redundant role in insulin secretion in pancreatic beta cells. J. Biol. Chem. 282, 2707–2716.
Ueda, K., Kawano, J., Takeda, K., Yujiri, T., Tanabe, K., Anno, T., Akiyama, M., Nozaki, J., Yoshinaga, T., Koizumi, A., et al., 2005. Endoplasmic reticulum stress induces Wfs1 gene expression in pancreatic beta-cells via transcriptional activation. Eur. J. Endocrinol. 153, 167–176.
Yamada, T., Ishihara, H., Tamura, A., Takahashi, R., Yamaguchi, S., Takei, D., Tokita, A., Satake, C., Tashiro, F., Katagiri, H., et al., 2006. WFS1-deficiency increases endoplasmic reticulum stress, impairs cell cycle progression and triggers the apoptotic pathway specifically in pancreatic beta-cells. Hum. Mol. Genet. 15, 1600–1609.
Yosida, M., Dezaki, K., Uchida, K., Kodera, S., Lam, N.V., Ito, K., Rita, R.S., Yamada, H., Shimomura, K., Ishikawa, S.E., et al., 2014. Involvement of cAMP/EPAC/TRPM2 activation in glucose- and incretin-induced insulin secretion. Diabetes 63, 3394–3403.
Wang, H., Ishizaki, R., Xu, J., Kasai, K., Kobayashi, E., Gomi, H., Izumi, T., 2013. The Rab27a effector exophilin7 promotes fusion of secretory granules that have not been docked to the plasma membrane. Mol. Biol. Cell 24, 319–330.